Fifth-Order Three-Pulse Scattering Spectroscopy: Can We Separate Homogeneous and Inhomogeneous Contributions to Optical Spectra?

Minhaeng Cho* and Graham R. Fleming*

Department of Chemistry and the James Franck Institute, The University of Chicago, 5735 S. Ellis Avenue, Chicago, Illinois 60637

Received: October 18, 1993; In Final Form: December 22, 1993®

A theoretical description of a new experimental technique related to the fifth-order optical nonlinearity of a chromophore in condensed media is presented. Three optical pulses are used to create three consecutive electronic coherence states the duration of the first two of which are controlled. Four nonlinear response functions representative of the full set of 16 response functions are calculated. The wave vectors associated with these four nonlinear response functions are given by $\mathbf{k}_1$, $2\mathbf{k}_3-\mathbf{k}_1$, $2\mathbf{k}_3-2\mathbf{k}_2+\mathbf{k}_1$, and $2\mathbf{k}_2-\mathbf{k}_1$. We consider a Gaussian function for the inhomogeneous distribution of electronic transition energies and express the fifth-order three-pulse scattering (FOTS) signals in terms of homogeneous and inhomogeneous contributions. If the two delay times controlling the coherence periods are set equal, the "diagonal" signal appearing with wave vector $2\mathbf{k}_3-2\mathbf{k}_2+\mathbf{k}_1$ allows a clean separation of homogeneous and inhomogeneous broadening for a Markovian line broadening function with arbitrary inhomogeneous width. For non-Markovian line broadening functions, the diagonal FOTS signal is free of short-time distortion from the Gaussian components, but in this case, both diagonal and off-diagonal (i.e. unequal delay times) signals must be measured to obtain the homogeneous and inhomogeneous contributions. We illustrate the results in the Markovian limit and provide a preliminary discussion of the situation for non-Markovian line broadening functions. The short-time behavior is discussed and a more general model in which the bath is described as a set of harmonic oscillators characterized by a spectral density is outlined.

1. Introduction

Electronic spectra of chromophores in condensed media are usually broad and often featureless. The broadening arises from thermal congestion, fluctuations of the electronic transition frequency caused by rapid fluctuations of the surrounding system (referred to as homogeneous broadening)[1] and inhomogeneously distributed slowly varying local solvent configurations.[2] The last two contributions originate from two different aspects of the solvent. The homogeneous broadening is related to the dynamical evolution of the solvation energy induced by the fluctuation of the solvent molecules. On the other hand, the inhomogeneous broadening results from the distribution of local configurations around each chromophore. It is often difficult to clearly separate the two contributions in liquids, since the time scales of the local structural transitions may be quite similar to those of the solvent fluctuations. Both the dynamical aspects of the solvent–solute interaction, which result in the homogeneous contribution to the optical spectrum, and the inhomogeneous distribution play important roles in chemical dynamics in condensed media.[3,4] In addition, the inhomogeneous distribution of the electronic transition energy is an interesting quantity which can be studied from the equilibrium statistical mechanics of liquids.[5-9]

In order to eliminate the effect of inhomogeneous dephasing, photon echo measurements have been used.[10-13] For example, consider a two-pulse photon echo measurement for which the pulse configuration is shown in Figure 1. The first external field whose wave vector is $\mathbf{k}_1$ creates an electronic coherence state. After a controlled delay time, τ_1, a second electronic coherence state is created by two interactions with a second external field propagating with wave vector $\mathbf{k}_2$. The second electronic coherence state evolves for time t. If there is a broad inhomogeneous distribution of the electronic transition energies of chromophores in condensed media, the rephasing process makes the echo intensity with wave vector $2\mathbf{k}_2-\mathbf{k}_1$ peak at $t=\tau_1$.[10,11,14] Photon echo signals are usually measured by integrating the echo intensity over time t (see Figure 1). Then the measured signal can be written as

$$S_{PE}(\tau_1) \propto \int_0^\infty dt\, H(\tau_1,t)I(\tau_1-t) \qquad (1)$$

where $H(\tau_1,t)$ and $I(\tau_1,t)$ denote the homogeneous and inhomogeneous echo response functions. The inhomogeneous part is usually given by the ensemble average of the inhomogeneous electronic phase. If the inhomogeneous distribution is very broad compared to any time scale of the nuclear dynamics, $I(\tau_1,t)$ can be approximated by a δ function, $\delta(\tau_1-t)$. Thus the echo signal is completely determined by the homogeneous part of the total response contribution, $H(\tau_1,\tau_1)$. For example, if we invoke the Markovian approximation to the solvent fluctuation correlation function, then $H(\tau_1,\tau_1)=\exp\{-4\Gamma\tau_1\}$, where Γ is the pure dephasing constant. As discussed by the authors,[14] although the homogeneous contribution $H(\tau_1,t)$ in real molecular liquids is likely to be more complicated than implied by the Markovian limit, if $I(\tau_1,t)\sim\delta(\tau_1-t)$, the echo signal is still governed by the homogeneous contribution alone. However, if the inhomogeneous width is comparable to the inverse of the time scale of the nuclear dynamics (but is still static), the echo signal given

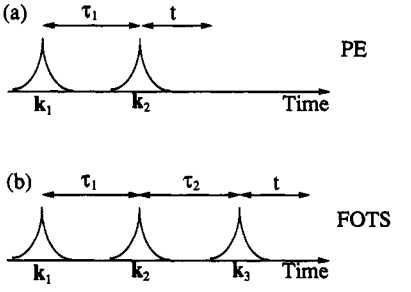

Figure 1. Pulse sequences for two-pulse photon echo (PE) and fifth-order three-pulse scattering (FOTS). $\mathbf{k}_i$ and τ_i denote the wave vector of the ith pulse and the controlled delay time between the ith and $(i+1)$ pulses, respectively.

® Abstract published in *Advance ACS Abstracts*, March 1, 1994.

0022-3654/94/2098-3478$04.50/0

by an integral over t contains both homogeneous and inhomogeneous contributions and simply does not represent the homogeneous contribution. The measured photon echo signals cannot be, therefore, distinguished from three-pulse scattering signals[15] or spatial- and frequency-grating spectroscopies[16] experimentally.

In order to overcome this barrier, we propose a new experiment utilizing three pulses propagating with different wave vectors (see Figure 1). The basis of the new experiment is the introduction of a second coherence period whose duration is controllable. As we will show, this can be achieved at fifth order (six-wave mixing) using a configuration involving three pulses with different wave vectors. The experiment now becomes "two dimensional", and both diagonal ($\tau_1 = \tau_2$) and off-diagonal ($\tau_1 \neq \tau_2$) contributions can be recorded.

The above considerations apply when the inhomogeneous contribution is truly static. In the case of more general stochastic models of liquid dynamics, the distribution between homogeneous and inhomogeneous broadening becomes blurred or even meaningless. However, there are many circumstances when we expect a significant contribution to the spectral broadening that is effectively static. Examples include solutes in polar solvents, at either reduced temperature[17] or high viscosity,[18,19] and chromophores in proteins such as light harvesting systems.[20]

Instead of considering the general fifth-order response functions discussed by Tanimura and Mukamel,[21] we focus specifically on the case where three pulses create three consecutive electronic coherence states and the duration times of pulses are sufficiently short to ignore the population evolution during the pulse duration times. This is a reasonable assumption, since the population evolution is generally slow on the femtosecond time scale. Four-wave mixing spectroscopy with the same pulse configuration is called three-pulse scattering spectroscopy.[15] We thus call the six-wave mixing spectroscopy we propose here fifth-order three-pulse scattering spectroscopy (FOTS). Our goal is to show that the FOTS measurements can be used to measure both the homogeneous and inhomogeneous contributions. As we shall show later, one of the FOTS signals with wave vector $2\mathbf{k}_3 - 2\mathbf{k}_2 + \mathbf{k}_1$, when measured under the condition $\tau_1 = \tau_2$ (diagonal contribution), allows this separation to be made clearly in the Markovian limit even though the scattered field is integrated over time. The situation is more complicated when more general, non-Markovian, line broadening functions are used. Even in this case, the short-time distortion of the standard echo signal resulting from Gaussian contributions to the line broadening is eliminated in the diagonal signal. However, both diagonal and off-diagonal ($\tau_1 \neq \tau_2$) parts of the signal must be measured to distinguish between dynamical and static line broadening mechanisms. The off-diagonal signal contribution contains both contributions, and so a combination of both measurements will also allow determination of the width of the inhomogeneous distribution of electronic transition energies.

A key difference of the FOTS experiment from lower-order spectroscopies is that the two electronic coherence periods are arbitrarily controlled, whereas both two-pulse or three-pulse photon echoes involve two electronic coherence periods, but only the duration of the first one of the two is controllable. If the signal is measured by integrating over the second electronic coherence period, information on the rephasing process is lost if the rephasing is not perfectly completed because of the finite inhomogeneous width. On the other hand, in the FOTS measurements each of the two consecutive electronic coherence periods is arbitrarily and independently controllable. Therefore the rephasing process can be directly monitored by two-dimensional measurements (with two variable delay times). This additional degree of freedom available for controlling electronic coherence duration times distinguishes FOTS experiments from third-order (four-wave mixing) spectroscopies, i.e. photon echoes, pump-probe.

Recently, Tanimura and Mukamel[22] suggested a very interesting fifth-order off-resonant spectroscopy using two pairs of excitation pulses and a probe pulse. They showed that this two-dimensional measurement can separate the inhomogeneous distribution of slowly varying parameters, for example of local liquid configurations, from the total spectral distribution of dynamical time scales. FOTS spectroscopy differs from their proposed experiment by utilizing resonant optical fields and by directly measuring the response of solute to both dynamical and static features of the solvent.

We organize the paper as follows. Response functions for the FOTS spectroscopies are given in section 2. A few simple cases for the line broadening functions are considered in section 3. Assuming that a collection of harmonic oscillators are effectively coupled to the electronic transitions, the homogeneous line broadening functions are given in terms of the correctly weighted spectral density in section 4. We summarize the results and provide a brief physical picture of the new technique in section 5.

2. Response Functions for Fifth-Order Three-Pulse Scattering Spectroscopy

We consider a molecule with two electronic states, $|g\rangle$ and $|e\rangle$. The molecular Hamiltonian is

$$H_0 = |g\rangle H_g \langle g| + |e\rangle (H_e + \omega_{eg}) \langle e| \tag{2}$$

ω_{eg} is the electronic energy gap between the two states. H_g and H_e denote diabatic nuclear Hamiltonians of the electronic ground and excited states, respectively. The electronic energy gap in condensed media fluctuates due to the interaction with the bath. Thus we shall assume[14]

$$\omega_{eg}(t) = \bar{\omega}_{eg} + \epsilon + \delta\omega(t) \tag{3}$$

where $\bar{\omega}_{eg}$ is the electronic energy gap averaged over all the chromophores. ϵ for a particular chromophore represents a deviation from $\bar{\omega}_{eg}$ and is not time-dependent. Finally, $\delta\omega(t)$ denotes a fluctuating variable around $\bar{\omega}_{eg} + \epsilon$.

The external field is given by

$$E(\mathbf{r},t) = E_1(t + \tau_1 + \tau_2) \exp(i\mathbf{k}_1\mathbf{r} - i\omega t) + E_2(t + \tau_2) \exp(i\mathbf{k}_2\mathbf{r} - i\omega t) + E_3(t) \exp(i\mathbf{k}_3\mathbf{r} - i\omega t) + \text{complex conjugates} \tag{4}$$

where $E_i(t)$ and ω denote the temporal amplitude and mean frequency of the ith incident pulse. For simplicity we consider that the frequencies of the three external fields are all equal (degenerate six-wave mixing spectroscopy). The first, second, and third pulses peak at times $-(\tau_1 + \tau_2)$, $-\tau_2$, and 0, respectively (see Figure 1). τ_1 and τ_2 are the relative delays of the pulses. The total Hamiltonian is then

$$H = H_0 - \mu E(\mathbf{r},t) \tag{5}$$

where μ is the electric dipole operator, which is coordinate-independent (Condon approximation)

$$\mu = |e\rangle \mu_{eg} \langle g| + |g\rangle \mu_{ge} \langle e| \tag{6}$$

Considering $\mu E(\mathbf{r},t)$ as a perturbation term and expanding the density matrix up to the fifth-order, we find the fifth-order nonlinear polarization

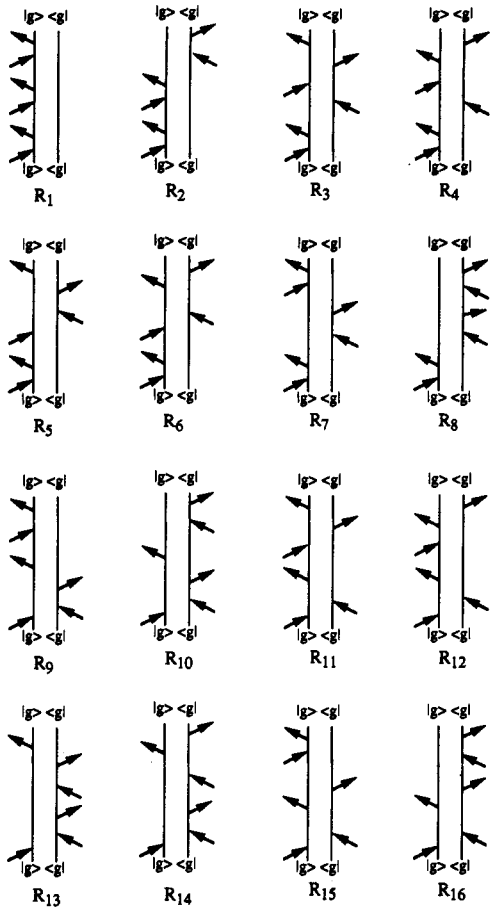

Figure 2. Double-sided Feynman diagrams for the 16 response functions. The corresponding expressions are given in Appendix A.

$$P^{(5)}(\mathbf{r},t) = [\prod_{j=1}^{5}\int_0^\infty dt_j]S^{(5)}(t_5,t_4,t_3,t_2,t_1)[\prod_{j=1}^{5}E(\mathbf{r},t-\sum_{k=j}^{5}t_k)] \quad (7)$$

Here $S^{(5)}$ represents the fifth-order nonlinear response function, which consists of 32 terms distinguished by their Liouville space pathways

$$S^{(5)}(t_5,t_4,t_3,t_2,t_1) = 2Im\sum_{\alpha=1}^{16}R_\alpha(t_5,t_4,t_3,t_2,t_1) \quad (8)$$

In Appendix A, we list the 16 nonlinear response functions. The other 16 response functions are given by the complex conjugates of the given terms. The corresponding double-sided Feynman diagrams are shown in Figure 2. To see the physical meaning of the double-sided Feynman diagrams, consider the first diagram corresponding to the nonlinear response function R_1 given by $\mathrm{Tr}[G_{eg}(t_5)\,G_{gg}(t_4)\,G_{eg}(t_3)\,G_{gg}(t_2)\,G_{eg}(t_1)\,\rho_g]$. By reading from right to left, the initial equilibrium ground-state population is switched into an electronic coherence state $|e\rangle\langle g|$ by an interaction with the external field. This electronic coherence state then propagates for time t_1. During t_2, the system evolves as a population state $|g\rangle\langle g|$ on the potential energy surface of the electronic ground state. Next the electronic coherence state $|e\rangle\langle g|$ created by the third interaction with the external field evolves for t_3. The fourth interaction creates another population state $|g\rangle\langle g|$, which evolves for t_4. The last period, t_5, is the duration time of the electronic coherence state $|e\rangle\langle g|$.

A. Fifth-Order Three-Pulse Scattering (FOTS) Spectroscopy. We now consider a special case when the first pulse (with wave vector $\mathbf{k}_1$) interacts with the optical chromophore once, to create an electronic coherence state. Then the second pulse with wave vector $\mathbf{k}_2$ interacts twice with the chromophore to create the second electronic coherence state. Finally the two interactions with the third pulse with wave vector $\mathbf{k}_3$ generate the third electronic coherence state. In other words, this particular set of polarizations depend to the first order on E_1 and to the second order on E_2 and E_3. This particular sequence of interactions is what we earlier called the fifth-order three-pulse scattering (FOTS) experiment. Although the scheme we described above is a special case of the six-wave mixing spectroscopies, it should not be very difficult to consider more general, arbitrary-order nonlinear spectroscopies.[21] We find that the fifth-order scattering experiment we shall discuss shows clearly the advantage of the six-wave mixing spectroscopy over four-wave mixing techniques in separating the homogeneous and inhomogeneous contributions to the optical broadening.

TABLE 1: Nonlinear Response Functions and Corresponding Phase-Matching Conditions for Fifth-Order Three-Pulse Scattering (FOTS) Spectroscopy

$\Phi_1(t_5,t_4,t_3,t_2,t_1)$	$\Phi_2(t_5,t_4,t_3,t_2,t_1)$	$\Phi_3(t_5,t_4,t_3,t_2,t_1)$	$\Phi_4(t_5,t_4,t_3,t_2,t_1)$
R_1	R_2	R_3	R_4
R_5	R_6	R_7	R_8
R_9	R_{10}	R_{11}	R_{12}
R_{13}	R_{14}	R_{15}	R_{16}
$\mathbf{k}_1$	$2\mathbf{k}_3-\mathbf{k}_1$	$2\mathbf{k}_3-2\mathbf{k}_2+\mathbf{k}_1$	$2\mathbf{k}_2-\mathbf{k}_1$

Invoking the rotating wave approximation (RWA) and considering the associated phase-matching conditions, we can separate the 16 response functions into four groups, Φ_1–Φ_4, as listed in Table 1. The wave vectors of the fifth-order polarization within the rotating wave approximation are $\mathbf{k}_1$, $2\mathbf{k}_3-\mathbf{k}_1$, $2\mathbf{k}_3-2\mathbf{k}_2+\mathbf{k}_1$, and $2\mathbf{k}_2-\mathbf{k}_1$ corresponding to the first, second, third, and fourth groups, respectively.

Now we shall assume that the pulse duration time is sufficiently short to ignore the population evolution during the pulse duration time, that is to say, we shall consider the following approximations

$$G_{\alpha\alpha}(t_2) = G_{\alpha\alpha}(t_4) \cong 1 \qquad (\alpha = g,e) \quad (9)$$

Usually this is a good approximation, since the evolution of the population states is slow on the time scale of the femtosecond laser pulses. Within this approximation, the four response functions belonging to the same group are all the same. Thus, the four representative nonlinear response functions are

$$\Phi_1(=R_1=R_5=R_9=R_{13}) \cong \mathrm{Tr}[G_{eg}(t)\,G_{eg}(\tau_2)\,G_{eg}(\tau_1)\,\rho_g]$$

$$\Phi_2(=R_2=R_6=R_{10}=R_{14}) \cong \mathrm{Tr}[G_{ge}(t)\,G_{eg}(\tau_2)\,G_{eg}(\tau_1)\,\rho_g]$$

$$\Phi_3(=R_3=R_7=R_{11}=R_{15}) \cong \mathrm{Tr}[G_{eg}(t)\,G_{ge}(\tau_2)\,G_{eg}(\tau_1)\,\rho_g]$$

$$\Phi_4(=R_4=R_8=R_{12}=R_{16}) \cong \mathrm{Tr}[G_{ge}(t)\,G_{ge}(\tau_2)\,G_{eg}(\tau_1)\,\rho_g] \quad (10)$$

Note that there are three electronic coherence periods. The first electronic coherence period is controlled by the delay time (τ_1) between the first and the second pulses, and the second electronic coherence period is controlled by τ_2. The third electronic coherence state evolves for time t. Since no population evolutions are involved in this measurement, there are no vibrational coherences (quantum beats) in contrast to pump-probe[23] or three-pulse photon echo[16] measurements. In section 3, we will briefly discuss the intramolecular vibrational contribution to FOTS measurements.

The nonlinear polarizations corresponding to the four nonlinear response functions are

$$P_1^{(5)}(\tau_1,\tau_2,t;\mathbf{k}_S=\mathbf{k}_1) \cong \Phi_1(t,0,\tau_2,0,\tau_1)$$

$$P_2^{(5)}(\tau_1,\tau_2,t;\mathbf{k}_S=2\mathbf{k}_3-\mathbf{k}_1) \cong \Phi_2(t,0,\tau_2,0,\tau_1)$$

$$P_3^{(5)}(\tau_1,\tau_2,t;\mathbf{k}_S = 2\mathbf{k}_3 - 2\mathbf{k}_2 + \mathbf{k}_1) \cong \Phi_3(t,0,\tau_2,0,\tau_1)$$

$$P_4^{(5)}(\tau_1,\tau_2,t;\mathbf{k}_S = 2\mathbf{k}_2 - \mathbf{k}_1) \cong \Phi_4(t,0,\tau_2,0,\tau_1) \quad (11)$$

The scattered signals generated by the fifth-order nonlinearity of the chromophore are, within the slowly varying amplitude approximation,[13b] then

$$S_1(\tau_1,\tau_2;\mathbf{k}_S = \mathbf{k}_1) \propto \int_0^\infty dt|\Phi_1(t,0,\tau_2,0,\tau_1)|^2$$

$$S_2(\tau_1,\tau_2;\mathbf{k}_S = 2\mathbf{k}_3 - \mathbf{k}_1) \propto \int_0^\infty dt|\Phi_2(t,0,\tau_2,0,\tau_1)|^2$$

$$S_3(\tau_1,\tau_2;\mathbf{k}_S = 2\mathbf{k}_3 - 2\mathbf{k}_2 + \mathbf{k}_1) \propto \int_0^\infty dt|\Phi_3(t,0,\tau_2,0,\tau_1)|^2$$

$$S_4(\tau_1,\tau_2;\mathbf{k}_S = 2\mathbf{k}_2 - \mathbf{k}_1) \propto \int_0^\infty dt|\Phi_4(t,0,\tau_2,0,\tau_1)|^2 \quad (12)$$

Thus, by calculating the nonlinear response functions given in eq 10, we can obtain the four signals.

In order to calculate the nonlinear response functions, we expand H_e around H_g and consider the time-dependent electronic transition energy to be given by eq 3. We can then rewrite the response functions in terms of time-ordered exponential functions of the energy-gap fluctuation operator. Using the cumulant expansion technique and considering terms up to second order, we find the four nonlinear response functions as follows:

$$\Phi_1(t,0,\tau_2,0,\tau_1) = \exp\{-i\tilde{\omega}_{eg}(\tau_1 + \tau_2 + t)\} \times \langle\exp\{-i\epsilon(\tau_1 + \tau_2 + t)\}\rangle_I \times \exp\{-g(\tau_1 + \tau_2 + t)\}$$

$$\Phi_2(t,0,\tau_2,0,\tau_1) = \exp\{-i\tilde{\omega}_{eg}(\tau_1 + \tau_2 - t)\}\langle\exp\{-i\epsilon(\tau_1 + \tau_2 - t)\}\rangle_I \times \exp\{-2g(\tau_1 + \tau_2) - 2\mathrm{Re}[g(t)] + g(\tau_1 + \tau_2 + t)\}$$

$$\Phi_3(t,0,\tau_2,0,\tau_1) = \exp\{-i\tilde{\omega}_{eg}(\tau_1 - \tau_2 + t)\}\langle\exp\{-i\epsilon(\tau_1 - \tau_2 + t)\}\rangle_I \times \exp\{-2g(\tau_1) - 4\mathrm{Re}[g(\tau_2)] - 2\mathrm{Re}[g(t)] + 2g(\tau_1 + \tau_2) + 2\mathrm{Re}[g(\tau_2 + t)] - g(\tau_1 + \tau_2 + t)\}$$

$$\Phi_4(t,0,\tau_2,0,\tau_1) = \exp\{-i\tilde{\omega}_{eg}(\tau_1 - \tau_2 - t)\}\langle\exp\{-i\epsilon(\tau_1 - \tau_2 - t)\}\rangle_I \times \exp\{-2g(\tau_1) - 2\mathrm{Re}[g(\tau_2 + t)] + g(\tau_1 + \tau_2 + t)\} \quad (13)$$

Here the angle brackets $\langle\ \rangle_I$ denote an ensemble average over the inhomogeneous distribution,

$$\langle A\rangle_I = \int_{-\infty}^{\infty} d\epsilon\, A f(\epsilon) \quad (14)$$

where $f(\epsilon)$ represents the distribution function of the inhomogeneity parameter, ϵ. The line broadening function $g(t)$ is defined as

$$g(t) = \int_0^t ds_1 \int_0^{s_1} ds_2 \langle\delta\omega(s_1)\,\delta\omega(s_2)\rangle \quad (15)$$

where $\langle\delta\omega(s_1)\,\delta\omega(s_2)\rangle$ is a one-sided quantum correlation function, which is a complex function. In order to obtain eq 13, we introduced the factorization approximation to the trace operator. Because of the inhomogeneous effects, e.g. $\langle\exp\{-i\epsilon(\tau_1 + \tau_2 + t)\}\rangle_I$, the nonlinear response functions are peaked around $t = 0$, $\tau_1 + \tau_2$, $\tau_2 - \tau_1$ (when $\tau_2 > \tau_1$) or 0 (when $\tau_2 < \tau_1$), and $\tau_1 - \tau_2$ (when $\tau_1 > \tau_2$) or 0 (when $\tau_1 < \tau_2$) corresponding to Φ_1–Φ_4, respectively.

In practice, the wave vector ($\mathbf{k}_1$) of S_1 is identical to those of the first pulse and one of the four-wave spatial grating signals,[14] and the wave vector of S_4 is identical to that of the conventional two-pulse photon echo field.[16] Therefore, it is difficult to distinguish the sixth-order signal from the lower-order signals in these two cases. However, the wave vectors of the two components corresponding to Φ_2 and Φ_3 are clearly separated from the lower-order signals and thus can be measured without any complications from those of the lower-order contributions. Therefore, we shall consider only S_2 and S_3 hereafter. Inserting Φ_2 and Φ_3 into eq 12, we have

$$S_2(\tau_1,\tau_2;\mathbf{k}_S = 2\mathbf{k}_3 - \mathbf{k}_1) \propto \int_0^\infty dt|\langle\exp\{-i\epsilon(\tau_1 + \tau_2 - t)\}\rangle_I|^2 \times \exp\{-4\mathrm{Re}[g(\tau_1 + \tau_2)] - 4\mathrm{Re}[g(t)] + 2\mathrm{Re}[g(\tau_1 + \tau_2 + t)]\}$$

$$S_3(\tau_1,\tau_2;\mathbf{k}_S = 2\mathbf{k}_3 - 2\mathbf{k}_2 + \mathbf{k}_1) \propto \int_0^\infty dt|\langle\exp\{-i\epsilon(\tau_1 - \tau_2 + t)\}\rangle_I|^2 \times \exp\{-4\mathrm{Re}[g(\tau_1)] - 8\mathrm{Re}[g(\tau_2)] - 4\mathrm{Re}[g(t)] + 4\mathrm{Re}[g(\tau_1 + \tau_2)] + 4\mathrm{Re}[g(\tau_2 + t)] - 2\mathrm{Re}[g(\tau_1 + \tau_2 + t)]\} \quad (16)$$

Equation 16 is the main result of this section. The FOTS signals consist of both inhomogeneous and homogeneous contributions. In general, the imaginary part of the line broadening function, $g(t)$, is related to the spectral diffusion. However, since only the real part of $g(t)$ appears in the signal, spectral diffusion does not affect the FOTS signal. For the sake of simplicity, we assume that the inhomogeneous distribution function $f(\epsilon)$ is Gaussian,

$$f(\epsilon) = f_0 \exp\{-\epsilon^2/2\Delta^2\} \quad (17)$$

where f_0 is a weighting factor. Then the inhomogeneous factors in eq 16 are respectively

$$|\langle\exp\{-i\epsilon(\tau_1 + \tau_2 - t)\}\rangle_I|^2 = 2\pi f_0^2\Delta^2 \exp\{-\Delta^2(\tau_1 + \tau_2 - t)^2\} \quad \text{for } S_2$$

$$|\langle\exp\{-i\epsilon(\tau_1 - \tau_2 + t)\}\rangle_I|^2 = 2\pi f_0^2\Delta^2 \exp\{-\Delta^2(\tau_1 - \tau_2 + t)^2\} \quad \text{for } S_3 \quad (18)$$

Since the line broadening function $g(t)$ is usually very complicated, except for the Markovian limit (Bloch approximation),[14] we cannot obtain analytic expressions for S_2 and S_3 by evaluating the integral over t. We consider several limiting cases before discussing the general response.

3. FOTS Signals with Approximate Line Broadening Functions

In this section, we shall consider three limiting cases: (i) broad inhomogeneous limit, (ii) Markovian limit (optical Bloch approximation), and (iii) Gaussian broadening limit (short-time approximation). Although each of them is a limiting case, since the exact analytic expressions can be obtained in these limits, we find that each case is revealing in understanding the nature of FOTS experiments.

A. Inhomogeneous Broadening Limit. In case of the large inhomogeneous broadening limit, the inhomogeneity factors can be approximated as δ functions, $\delta(\tau_1 + \tau_2 - t)$ and $\delta(\tau_1 - \tau_2 + t)$. The signals then reduce to

$$S_2(\tau_1,\tau_2;\mathbf{k}_S = 2\mathbf{k}_3 - \mathbf{k}_1) \propto \exp\{-8\mathrm{Re}[g(\tau_1 + \tau_2)] + 2\mathrm{Re}[g(2\tau_1 + 2\tau_2)]\}$$

$$S_3(\tau_1,\tau_2;\mathbf{k}_S = 2\mathbf{k}_3 - 2\mathbf{k}_2 + \mathbf{k}_1) \propto \exp\{-4\mathrm{Re}[g(\tau_1)] - 8\mathrm{Re}[g(\tau_2)] - 4\mathrm{Re}[g(\tau_2 - \tau_1)]\} \times \exp\{4\mathrm{Re}[g(\tau_1 + \tau_2)] + 4\mathrm{Re}[g(2\tau_2 - \tau_1)] - 2\mathrm{Re}[g(2\tau_2)]\} \text{ for } \tau_2 \geq \tau_2 \quad (19)$$

Note that the integral over t in eq 16 ranges from 0 to ∞. Thus, the signal S_3 is given by eq 19 only when $\tau_2 \geq \tau_1$. In this broad

inhomogeneous limit, the inhomogeneous contribution is completely eliminated by perfect rephasing processes. However, in this case conventional photon echo measurements also give the homogeneous dephasing behavior. Therefore, FOTS measurements do not show any merits in this limit.

B. Markovian Limit (Optical Bloch Approximation). Although the Markovian approximation to the fluctuation correlation function in eq 15 was shown to be poor in liquids,[11b,12b,14] in order to understand the distinguishability of the inhomogeneous and homogeneous contributions, we consider the Markovian limit. In this case the line broadening function $g(t)$ is simply given by $g(t) = \Gamma t$. Within this approximation we can evaluate the integral for S_2 and S_3,

$$S_2(\tau_1,\tau_2;\mathbf{k}_S = 2\mathbf{k}_3 - \mathbf{k}_1) \propto C_0 \exp\{-4\Gamma(\tau_1 + \tau_2)\} \operatorname{erfc}\{\Gamma/\Delta - \Delta(\tau_1 + \tau_2)\}$$

$$S_3(\tau_1,\tau_2;\mathbf{k}_S = 2\mathbf{k}_3 - 2\mathbf{k}_1) \propto C_0 \exp\{-4\Gamma\tau_2\} \operatorname{erfc}\{\Gamma/\Delta - \Delta(\tau_2 - \tau_1)\} \quad \text{for } \tau_2 \geq \tau_1 \quad (20)$$

where $C_0 = \pi^{3/2} f_0^2 \Delta \exp\{\Gamma^2/\Delta^2\}$. Here $\operatorname{erfc}(x)$ is the complementary error function, $1 - \operatorname{erf}(x)$. In the case of (i) the broad inhomogeneous limit ($\Delta \gg \Gamma$) and (ii) short delay time $\Delta \gg 1/|\tau_2 \pm \tau_1|$, $\operatorname{erfc}(x)$ is approximately equal to $2 - \exp(-x^2)/x\sqrt{\pi}$. Then the two signals S_2 and S_3 are simply

$$S_2(\tau_1,\tau_2;\mathbf{k}_S = 2\mathbf{k}_3 - \mathbf{k}_1) \propto \exp\{-4\Gamma(\tau_1 + \tau_2)\}$$

$$S_3(\tau_1,\tau_2;\mathbf{k}_S = 2\mathbf{k}_3 - 2\mathbf{k}_2 + \mathbf{k}_1) \propto \exp\{-4\Gamma\tau_2\} \quad \text{for } \tau_2 \geq \tau_1 \quad (21)$$

These two equations can also be obtained from eq 19 by invoking the Markovian approximation. However, if either of the above limits (i) and (ii) is not satisfied, we have additional contributions from the inhomogeneous effects appearing in the complementary error functions. Consider two-dimensional measurements of S_2 and S_3 by varying τ_1 and τ_2 independently. The diagonal parts of the two-dimensional signals (when $\tau = \tau_1 = \tau_2$) are respectively

$$S_2(\tau = \tau_1 = \tau_2;\ \mathbf{k}_S = 2\mathbf{k}_3 - \mathbf{k}_1) \propto C_0 \exp\{-8\Gamma\tau\} \operatorname{erfc}\{\Gamma/\Delta - 2\Delta\tau\}$$

$$S_3(\tau = \tau_1 = \tau_2;\ \mathbf{k}_S = 2\mathbf{k}_3 - 2\mathbf{k}_2 + \mathbf{k}_1) \propto C_0 \operatorname{erfc}\{\Gamma/\Delta\} \exp\{-4\Gamma\tau\} \quad (22)$$

As can be seen in eq 22, the diagonal part of S_3 is purely determined by the homogeneous contribution, even though no restrictions were placed on the time scale of the inhomogeneous broadening function. In contrast, the diagonal part of S_2 still consists of both homogeneous and inhomogeneous contributions.

Consider a special case of S_3 when $\Delta \gg \Gamma$ and $\Delta \ll 1/\delta\tau$ with $\delta\tau = \tau_2 - \tau_1 \geq 0$. Although the short-time part of both S_2 and S_3 can, in general, be measured to get information on Δ, we find that the difference between the two delay times in the measurement of S_3 may be more easily controlled in the real experiment. In this limit, since $\operatorname{erfc}\{\Gamma/\Delta - \Delta(\tau_2 - \tau_1)\} \sim 1 + 2\Delta\delta\tau/\sqrt{\pi}$, we find the off-diagonal part of the signal, $S_3(\tau_1 \neq \tau_2)$:

$$S_3(\tau_1,\tau_2;\mathbf{k}_S = 2\mathbf{k}_3 - 2\mathbf{k}_2 + \mathbf{k}_1) \propto C_0 \exp\{-4\Gamma\tau_2\}\{1 + 2\Delta\delta\tau/\sqrt{\pi}\} \quad \text{with } \delta\tau = \tau_2 - \tau_1 \geq 0 \quad (23)$$

Therefore, for a fixed τ_2, by varying $\delta\tau$ and plotting the signal S_3 with respect to $\delta\tau$ for small $\delta\tau$, we can measure the width of the inhomogeneous distribution Δ directly from the slope of the plot. This ability to measure the width of the inhomogeneous distribution function is a unique feature of the S_3 measurement compared to measurements of S_2 or conventional photon echoes.

It should be mentioned that in the Markovian limit the line broadening function is linearly dependent on time arguments, e.g., $g(\tau_1 + \tau_2) = \Gamma(\tau_1 + \tau_2)$. Therefore, in this limit, a complete separation of the homogeneous contribution from the inhomogeneous effects can be achieved.

C. Gaussian (Inertial) Broadening Limit: Short-Time Behavior. An inertial component in the solvent fluctuations has been observed in time-dependent fluorescence Stokes shift measurements[24] and computer simulation studies.[25] The solvent fluctuation correlation function $\langle\delta\omega(t)\,\delta\omega(0)\rangle$ can be approximated by $\langle\delta\omega^2\rangle(1 - \Omega^2t^2/2 + \ldots)$ for short time. The initial quadratic decay constant is given as $\langle\delta\omega^2\rangle\Omega^2/2$. Then for a sufficiently short time, i.e. $\Omega^2t^2/2 \ll 1$, the line broadening function $g(t)$ is $\langle\delta\omega^2\rangle t^2/2$. In other words, on this time scale the whole system is intrinsically inhomogeneous regardless of a subsequent time scale separation between the homogeneous and inhomogeneous contributions. In this case it is not meaningful to separate Δ and $\sqrt{\langle\delta\omega^2\rangle}$. The magnitude $\sqrt{\Delta^2 + \langle\delta\omega^2\rangle}$ represents the width of the effective inhomogeneous distribution for short times. We shall discuss this point further in section 5. The FOTS signals S_2 and S_3 for very short times are

$$S_2(\tau_1,\tau_2;\mathbf{k}_S = 2\mathbf{k}_3 - \mathbf{k}_1) \propto \pi^{3/2} f_0^2 \frac{\Delta^2}{\Delta^2 + \langle\delta\omega^2\rangle} \operatorname{erfc}\{-\sqrt{\Delta^2 + \langle\delta\omega^2\rangle}(\tau_1 + \tau_2)\}$$

$$S_3(\tau_1,\tau_2;\mathbf{k}_S = 2\mathbf{k}_3 - 2\mathbf{k}_2 + \mathbf{k}_1) \propto \pi^{3/2} f_0^2 \frac{\Delta^2}{\Delta^2 + \langle\delta\omega^2\rangle} \operatorname{erfc}\{-\sqrt{\Delta^2 + \langle\delta\omega^2\rangle}(\tau_2 - \tau_1)\} \quad (24)$$

Both the diagonal and off-diagonal (measured with respect to $\delta\tau = \tau_2 - \tau_1$) signals decay as $\operatorname{erfc}(x)$ and give the magnitude of $\sqrt{\Delta^2 + \langle\delta\omega^2\rangle}$. It should be emphasized that eq 24 is valid only for short time, that is to say, the diagonal part of S_3 is a constant only for short time, since we did not include the term $\langle\delta\omega^2\rangle\Omega^2t^2/2$ in approximating $g(t)$ in this limit.

4. General Homogeneous Line Broadening Function: Effective Harmonic Bath Model

In this section we present a general model for the line broadening function. We shall assume that the bath consists of a large number of harmonic oscillators. The coupling strength of each harmonic oscillator to the electronic transition is determined by its displacement from the equilibrium position in the electronic ground state. The dimensionless displacement of the ith harmonic oscillator is defined as $\Gamma_i = m_i\omega_i\Delta_i^2/2\hbar$, where m_i, ω_i, and Δ_i are the mass, frequency, and displacement of the ith oscillator. The spectral density representing the dynamical aspects of the bath is then assumed to be represented by

$$\rho(\omega) \equiv \sum_i \Gamma_i\, \delta(\omega - \omega_i) \quad (25)$$

With the spectral density defined in eq 25, the line broadening function, $g(t)$, defined in eq 15 can be written as

$$g(t) = -i\bar{U}t + P(t) - iQ(t) \quad (26)$$

where

$$\bar{U} \equiv \int d\omega\, \omega\, \rho(\omega) \quad (27a)$$

$$P(t) \equiv \int d\omega\, \rho(\omega)[2n(\omega) + 1]\{1 - \cos\omega t\} \quad (27b)$$

$$Q(t) \equiv \int d\omega\, \rho(\omega) \sin\omega t \quad (27c)$$

Here $n(\omega)$ is the Bose-population factor, $1/\{\exp(\hbar\omega/k_BT) - 1\}$,

where k_B and T are the Boltzmann constant and temperature. $\bar{U}$ is equal to half of the Stokes shift magnitude. Various models, such as the stochastic model[1] or the Brownian oscillator model,[21] can be incorporated into the calculation by using suitable functional forms for the spectral density. Although the general line broadening function given in eq 26 is a complex function in time, only the real part of $g(t)$, $P(t)$, is needed to calculate the two FOTS signals in eq 16. Since the spectral shifts with respect to the delay times are described by the phase evolution of the response function, which is given by $Im[g(t)] = -\bar{U}t - Q(t)$, the FOTS signals given in eq 16 are not affected by spectral diffusion (solvation dynamics).

In order to understand the contributions to the FOTS signals from intramolecular vibrational modes, we assume that the spectral density $\rho(\omega)$ is divided into bath and high-frequency intramolecular vibrational modes, i.e. $\rho(\omega) = \rho_B(\omega) + \rho_V(\omega)$. Here $\rho_B(\omega)$ and $\rho_V(\omega)$ denote the spectral densities representing the distribution of the bath harmonic oscillators and intramolecular vibrational modes. Usually, the bath oscillators are distributed continuously because of the large number of degrees of freedom of the bath, whereas the intramolecular modes are discrete. The line broadening function $g(t)$ can then be written as $g(t) = g_B(t) + g_V(t)$. For simplicity, we consider one undamped intramolecular vibrational mode. The corresponding spectral density $\rho_V(\omega)$ is then given by $\rho_V(\omega) = \Gamma_V\,\delta(\omega - \omega_V)$, where $\Gamma_V (= m_V\omega_V\Delta_V^2/2\hbar)$ and ω_V are the coupling strength and vibrational frequency, respectively. The real part of the line broadening function of this intramolecular mode, $g_V(t)$, is equal to $\mathrm{Re}[g_V(t)] = \Gamma_V[2n(\omega_V) + 1]\{1 - \cos\omega_V t\}$. Since the total response function is given by an exponential of a sum of $\mathrm{Re}[g(t)]$'s and $\mathrm{Re}[g(t)] = \mathrm{Re}[g_B(t)] + \mathrm{Re}[g_V(t)]$, we can write the total response function as a product of the intramolecular and bath response functions

$$\Phi_\alpha(t,0,\tau_2,0,\tau_1) = \Phi_\alpha^B(t,0,\tau_2,0,\tau_1)\,\Phi_\alpha^V(t,0,\tau_2,0,\tau_1) \quad \text{for } \alpha = 1\text{–}4 \quad (28)$$

where $\Phi_\alpha^B(t,0,\tau_2,0,\tau_1)$ and $\Phi_\alpha^V(t,0,\tau_2,0,\tau_1)$ represent the bath and intramolecular mode response functions, respectively. Inserting the equations for $\mathrm{Re}[g_V(t)]$ into eq 16, we can write the two signals S_2 and S_3 as

$$S_2(\tau_1,\tau_2;\mathbf{k}_S = 2\mathbf{k}_3 - \mathbf{k}_1) \propto \int_0^\infty dt |\langle \exp\{-i\epsilon(\tau_1 + \tau_2 - t)\}\rangle_I|^2 \times \exp\{-4\mathrm{Re}[g_B(\tau_1 + \tau_2)] - 4\mathrm{Re}[g_B(t)] + 2\mathrm{Re}[g_B(\tau_1 + \tau_2 + t)]\} \times \exp\{-\Gamma_V(2n(\omega_V) + 1)[6 - 4\cos\omega_V(\tau_1 + \tau_2) - 4\cos\omega_V t + 2\cos\omega_V(\tau_1 + \tau_2 + t)]\} \quad (29)$$

$$S_3(\tau_1,\tau_2;\mathbf{k}_S = 2\mathbf{k}_3 - 2\mathbf{k}_2 + \mathbf{k}_1) \propto \int_0^\infty dt |\langle \exp\{-i\epsilon(\tau_1 - \tau_2 + t)\}\rangle_I|^2 \times \exp\{-4\mathrm{Re}[g_B(\tau_1)] - 8\mathrm{Re}[g_B(\tau_2)] - 4\mathrm{Re}[g_B(t)] + 4\mathrm{Re}[g_B(\tau_1 + \tau_2)] + 4\mathrm{Re}[g_B(\tau_2 + t)] - 2\mathrm{Re}[g_B(\tau_1 + \tau_2 + t)]\} \times \exp\{-\Gamma_V(2n(\omega_V) + 1)[10 - 4\cos\omega_V\tau_1 - 8\cos\omega_V\tau_2 - 4\cos\omega_V t + 4\cos\omega_V(\tau_1 + \tau_2) + 4\cos\omega_V(\tau_2 + t) - 2\cos\omega_V(\tau_1 + \tau_2 + t)]\} \quad (30)$$

The discrete intramolecular vibrational mode thus contributes to the signal as $\exp\{-A\cos\omega_V t\}$ with the constant A determined by the coupling strength Γ_V. However, since the oscillatory behavior induced by the intramolecular mode contribution is multiplied by the quickly decaying bath response function, it may be very difficult to observe the intramolecular vibrational dynamics in these two signals. This is in contrast to the three-pulse photon echo or pump-probe signals measuring the population evolution on both excited and ground electronic states, where the impulsively excited coherent vibrational contribution appears (in the small signal limit) as a cosinusoidal function, i.e. $\cos(\omega_V t + \phi_V)$, instead of $\exp\{-A\cos\omega_V t\}$.

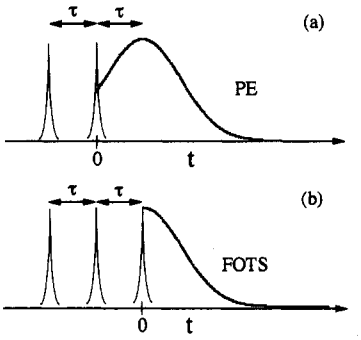

Figure 3. t-Dependent two-pulse photon echo and diagonal FOTS-S_3 signals (thick curves following the excitation pulses). The photon echo intensity is peaked at $t = \tau$, whereas the diagonal S_3 signal is peaked at $t = 0$ (see the text for details).

5. Discussion and Summary

We have described an experiment in which three optical pulses are used to create three consecutive electronic coherence states. The duration times of the first two electronic coherence periods are controlled by the two delay times between the pulses. The field scattered by the fifth-order optical nonlinearity is measured by integrating the scattering field intensity over the final coherence duration time. The fifth-order three-pulse scattering (FOTS) spectroscopies are divided into four groups, which are distinguished by different phase-matching conditions and different nonlinear response functions. The four wave vectors are $\mathbf{k}_1$, $2\mathbf{k}_3 - \mathbf{k}_1$, $2\mathbf{k}_3 - 2\mathbf{k}_2 + \mathbf{k}_1$, and $2\mathbf{k}_2 - \mathbf{k}_1$. The two components whose wave vectors are $2\mathbf{k}_3 - \mathbf{k}_1$ and $2\mathbf{k}_3 - 2\mathbf{k}_2 + \mathbf{k}_1$ are clearly distinguished from the lower-order spectroscopies.

A. Comparison of FOTS-S_3 Signal with Two-Pulse Photon Echo (TP-PE). In this subsection, we will consider S_3 only, which clearly showed some merits over S_2 and TP-PE measurements. In order to clarify the elimination of inhomogeneous effects in the FOTS (S_3) measurements observed along $2\mathbf{k}_3 - 2\mathbf{k}_2 + \mathbf{k}_1$, we compare it with the conventional two-pulse photon echo observed along $2\mathbf{k}_2 - \mathbf{k}_1$. Here we consider a finite inhomogeneous distribution.

The two pulses in the TP-PE measurement are separated by a controllable delay time τ as shown in Figure 3a, and the t-dependent photon echo intensity is shown by the thicker curve in the same figure. In this case, the second pulse acts as a time reverser for the inhomogeneous dephasing of the electronic coherence created by the first pulse. Because of the finite inhomogeneous width, the rephasing is not perfect; that is to say, the photon echo intensity is not a δ function with respect to t. However, the maximum of the t-dependent echo intensity still appears at $t = \tau$. It should be noted though that the echo intensity around the maximum is generally asymmetric. This arises because the homogeneous response function is a monotonously decreasing function with respect to t, whereas the inhomogeneous response function is Gaussian and thus symmetric around $t = \tau$. Thus the overall t-dependent echo intensity is asymmetric around the maximum. The t-dependent echo intensity is then determined by both the inhomogeneous and homogeneous responses. If the inhomogeneous width is very broad, the t-dependent echo intensity approaches a narrow δ-like function as a result of perfect rephasing. When the controllable time τ is set to zero, the t-dependent echo intensity is a monotonically decaying function, which is just the free-induction decay. When τ is comparable to $1/\Delta$, which is the time scale of the inhomogeneous effect, as shown in Figure 3a, the t-dependent echo intensity increases until it reaches the maximum ($t = \tau$) and decays by the free-induction decay. In this case the left-hand portion of the echo intensity is missing because of the causality condition. Now for a large $\tau \gg 1/\Delta$, the

full—from the left wing to the right wing—t-dependent echo intensity is included in the integration over t. Throughout these three cases, the overall homogeneous response decays with respect to any combinations of t and τ. The resulting τ-dependent echo signal is then obtained by calculating the area under the t-dependent echo intensity. Therefore, the τ-dependent integrated echo signal increases for short time ($\tau < 1/\Delta$), and after it reaches its maximum, the signal decays. Although this initial increasing behavior is governed by the time scale of the inhomogeneous effect, i.e. $1/\Delta$, the short-time Gaussian nature of the line broadening function discussed in section 3C is an inhomogeneous effect, where the corresponding quasi-inhomogeneous width is given by $\sqrt{\langle\delta\omega^2\rangle}$. When a Gaussian component of a line broadening function exists, the presence of an initial increase (Figure 3a) in the integrated two-pulse echo signal is likely to be an intrinsic characteristic of the integrated photon echo signal.

We now consider the FOTS-S_3 signal given in eq 16 with 18. For a finite inhomogeneous distribution, regardless of either the controlled delay time τ or the inhomogeneous width Δ, the t-dependent echo intensity is a monotonically decaying function, as illustrated in Figure 3b. This is not only because the rephasing is always completed by controlling the two delay times to be equal but also because causality requires the signal to begin only at the third pulse. This is the novel feature of the S_3 measurement. Therefore, the diagonal signal $S_3(\tau = \tau_1 = \tau_2)$ is not contaminated by the strong inhomogeneous effect which appears in the TP-PE measurements. However, a second complication arising from inhomogeneous effects is not eliminated by the diagonal FOTS-S_3 measurement. We discuss this topic in the following section. One other advantage of the S_3 measurement, aside from the possibility of measuring the homogeneous response function by making the rephasing perfect, is that we can also deliberately make the rephasing imperfect and measure the off-diagonal signal where $\tau_1 \neq \tau_2$. In the case when there is no inhomogeneous effect, for a fixed τ_1, the τ_2-dependent signal with $\tau_2 \geq \tau_1$ should have the same decay profile as the diagonal S_3 signal, since both are determined by the same homogeneous response. Thus, by measuring both the diagonal and off-diagonal signals, we may be able to determine the inhomogeneous width.

B. Can We Separately Measure Homogeneous and Inhomogeneous Contributions? When we discuss the homogeneous and inhomogeneous contributions, we have already assumed that there exists a significant time scale separation between the homogeneous and inhomogeneous effects on the fluctuation of the electronic transition energy gap. In general, such a separation may not exist. For example, if the local structures are rapidly interconverting with a frequency comparable to the frequencies of the solvent motions, there is no clear-cut division of homogeneous and inhomogeneous contributions. In this case the theoretical model must incorporate these two aspects simultaneously, in order to describe the energy gap fluctuations. Conceptually, there is no *static* inhomogeneous effect in this case. In this situation, experiments measuring the evolution of the electronic coherence state, such a photon echo, may not be superior to simple absorption spectroscopy. The reason (as discussed in section 5A) is that no portion of the full response function is eliminated by these experiments, which is in contrast to what we expect from the conventional photon echo measurements.

In this paper we have discussed whether photon echo measurements are useful to effectively eliminate the static inhomogeneous distribution when the width of the inhomogeneous distribution, Δ, is comparable to the homogeneous width, $\langle\delta\omega^2\rangle$. Our concern may appear to be inconsistent with a number of recent studies which have described absorption spectra in molecular liquids as being governed by large inhomogeneous contributions and having shapes close to Gaussian.[7,9,17] Do these observations mean there is a large static distribution of local structures around the chromophores? The distribution is certainly static on the time scale of the inverse line shape, but this does not imply that spectroscopies that are higher order than linear absorption cannot reveal the dynamical time scale. Absorption spectra at *high temperature* are in fact mostly determined by the short-time nature of the solvent dynamics because, via the fluctuation–dissipation theorem, the fluctuation amplitude is proportional to k_BT.

What the diagonal S_3 signal can do in the intermediate case when Δ is comparable to $\langle\delta\omega^2\rangle^{1/2}$ is to eliminate (vide supra) the short-time distortion caused by the Gaussian contribution to the response function (see section 3C). This contribution is associated with the inhomogeneous distribution of short-time snapshot local structures around chromophores. The contamination of the S_3 signal from inhomogeneous effects in the case of non-Markovian line broadening must now be discussed in more detail. To do so, we return to eq 30. When $\tau_1 = \tau_2$, the inhomogeneous factor for S_3 in eq 30 is $f_0 \exp(-\Delta^2 t^2)$, which is independent of $\tau_1 (= \tau_2)$. In case of the general bath model, the line broadening function, for example $g(\tau_2 + t)$, cannot be completely separated into a function of τ_2 only and a function of t only. Thus there is a possible contamination of the signal from the inhomogeneous effect because of this nonseparability. The inertial solvation dynamics[24,25] mentioned in section 3C provide a specific example where this may occur. Numerical calculations show that for such a case the contamination is much smaller in the diagonal FOTS-S_3 signal than in the standard two-pulse echo. In addition, within our model of two separate contributions to the overall line shape originating from homogeneous and static inhomogeneous effects (eq 3), the line broadening function $g(t)$ is solely determined by $\langle\delta\omega^2\rangle$, as can be seen in eq 15. This implies (and is confirmed by preliminary numerical studies) that the decay of the diagonal S_3 signal is largely determined by a function of the homogeneous fluctuation amplitude $\langle\delta\omega^2\rangle$, whereas the short-time off-diagonal S_3 signal can provide the whole fluctuation amplitude regardless of the time scale separation between homogeneous and inhomogeneous contributions. Thus, by carrying out both diagonal and off-diagonal measurements, it should be possible to characterize the separate contributions, $\langle\delta\omega^2\rangle$ and Δ^2, to the spectral broadening. The way in which the bath dynamics deviate from Gaussian dynamics can then be captured by the S_3 measurements. These non-Gaussian aspects of the response function, which are higher-order expansion terms with respect to time than the quadratic term in the $g(t)$'s, also contribute to the wings of the absorption spectrum.

We must close this discussion by noting that detailed numerical studies with a wide range of parameters are required to establish the limitations of the FOTS-S_3 measurement in the non-Markovian case. However, there exist numerous cases where many orders of magnitude separate the slow fluctuating variables, such as molecular conformations and local structures in glasses, from the fast fluctuating variables, such as collective intermolecular vibrations and phonons in proteins and glasses. In these cases the Markovian approximation may be well applicable. In this limit, the inhomogeneous contribution appears as a complementary error function with, for example, an argument, $(\Gamma/\Delta) - (\Delta(\tau_2 - \tau_1))$ for the FOTS signal with wave vector $2\mathbf{k}_3 - 2\mathbf{k}_2 + \mathbf{k}_1$. The diagonal part ($\tau_1 = \tau_2$) of this signal contains only the homogeneous contribution, even though the FOTS signals are obtained by integrating the scattered field intensity, as are conventional photon echo signals. The off-diagonal part ($\tau_1 \neq \tau_2$) of the same FOTS signal, when measured with respect to $\delta\tau = \tau_2 - \tau_1 \geq 0$, can be used to directly measure the width (Δ) of the inhomogeneous distribution function. At short times, the signals S_2 and S_3 decay like a complementary error function with negative arguments. By measuring the initial slope of signals at short time, it may be possible to estimate $\sqrt{\Delta^2 + \langle\delta\omega^2\rangle}$, where Δ and $\langle\delta\omega^2\rangle$ are the width of the inhomogeneous distribution and mean square solvent fluctuation amplitude.

Acknowledgment. Joshua Jortner's ideas have been a constant source of inspiration in our studies of chemical dynamics. We thank Prof. Shaul Mukamel for comments on the manuscript and for providing us with a preprint of ref 21 and Jae Young Yu for helpful discussions and preliminary numerical calculations. We thank the reviewers for insightful comments on the original manuscript. This work was supported by the National Science Foundation.

Appendix A. Nonlinear Response Functions for Six-Wave Mixing Spectroscopy

We deine the Liouville space propagator $G_{ab}(t)$ as

$$G_{ab}(t)A = \exp(-iH_a t)A \exp(iH_b t) \qquad \text{(A-1)}$$

where A is an arbitrary operator. The 16 response functions corresponding to the 16 Liouville space pathways shown in Figure 2 are given as

$$R_1 = \mathrm{Tr}[G_{eg}(t_5)\, G_{gg}(t_4)\, G_{eg}(t_3)\, G_{gg}(t_2)\, G_{eg}(t_1)\, \rho_g]$$

$$R_2 = \mathrm{Tr}[G_{ge}(t_5)\, G_{gg}(t_4)\, G_{eg}(t_3)\, G_{gg}(t_2)\, G_{eg}(t_1)\, \rho_g]$$

$$R_3 = \mathrm{Tr}[G_{eg}(t_5)\, G_{ee}(t_4)\, G_{ge}(t_3)\, G_{gg}(t_2)\, G_{eg}(t_1)\, \rho_g]$$

$$R_4 = \mathrm{Tr}[G_{ge}(t_5)\, G_{ee}(t_4)\, G_{ge}(t_3)\, G_{gg}(t_2)\, G_{eg}(t_1)\, \rho_g]$$

$$R_5 = \mathrm{Tr}[G_{eg}(t_5)\, G_{ee}(t_4)\, G_{eg}(t_3)\, G_{gg}(t_2)\, G_{eg}(t_1)\, \rho_g]$$

$$R_6 = \mathrm{Tr}[G_{ge}(t_5)\, G_{ee}(t_4)\, G_{eg}(t_3)\, G_{gg}(t_2)\, G_{eg}(t_1)\, \rho_g]$$

$$R_7 = \mathrm{Tr}[G_{eg}(t_5)\, G_{gg}(t_4)\, G_{ge}(t_3)\, G_{gg}(t_2)\, G_{eg}(t_1)\, \rho_g]$$

$$R_8 = \mathrm{Tr}[G_{ge}(t_5)\, G_{gg}(t_4)\, G_{ge}(t_3)\, G_{gg}(t_2)\, G_{eg}(t_1)\, \rho_g]$$

$$R_9 = \mathrm{Tr}[G_{eg}(t_5)\, G_{gg}(t_4)\, G_{eg}(t_3)\, G_{ee}(t_2)\, G_{eg}(t_1)\, \rho_g]$$

$$R_{10} = \mathrm{Tr}[G_{ge}(t_5)\, G_{gg}(t_4)\, G_{eg}(t_3)\, G_{ee}(t_2)\, G_{eg}(t_1)\, \rho_g]$$

$$R_{11} = \mathrm{Tr}[G_{eg}(t_5)\, G_{ee}(t_4)\, G_{ge}(t_3)\, G_{ee}(t_2)\, G_{eg}(t_1)\, \rho_g]$$

$$R_{12} = \mathrm{Tr}[G_{ge}(t_5)\, G_{ee}(t_4)\, G_{ge}(t_3)\, G_{ee}(t_2)\, G_{eg}(t_1)\, \rho_g]$$

$$R_{13} = \mathrm{Tr}[G_{eg}(t_5)\, G_{ee}(t_4)\, G_{eg}(t_3)\, G_{ee}(t_2)\, G_{eg}(t_1)\, \rho_g]$$

$$R_{14} = \mathrm{Tr}[G_{ge}(t_5)\, G_{ee}(t_4)\, G_{eg}(t_3)\, G_{ee}(t_2)\, G_{eg}(t_1)\, \rho_g]$$

$$R_{15} = \mathrm{Tr}[G_{eg}(t_5)\, G_{gg}(t_4)\, G_{ge}(t_3)\, G_{ee}(t_2)\, G_{eg}(t_1)\, \rho_g]$$

$$R_{16} = \mathrm{Tr}[G_{ge}(t_5)\, G_{gg}(t_4)\, G_{ge}(t_3)\, G_{ee}(t_2)\, G_{eg}(t_1)\, \rho_g] \qquad \text{(A-2)}$$

where ρ_g is the thermal density matrix,

$$\rho_g = \exp(-H_g/k_BT)/\mathrm{Tr}[\exp(-H_g/k_BT)] \qquad \text{(A-3)}$$

Here we assumed that the system is initially in thermal equilibrium in the ground state.

References and Notes

(1) Kubo, R. *Adv. Chem. Phys.* **1969**, *15*, 101.
(2) Birks, J. B. *Photophysics of Aromatic Molecules*; Wiley: New York, 1970.
(3) Rips, I.; Jortner, J. *J. Chem. Phys.* **1987**, *87*, 2090. Rips, I.; Jortner, J. *Chem. Phys. Lett.* **1987**, *133*, 411. Bixon, M.; Jortner, J. *J. Phys. Chem.*, in press.
(4) Onuchic, J. N.; Wolynes, P. G. *J. Chem. Phys.* **1988**, *92*, 6495.
(5) Griem, H. R. *Spectral Line Broadening by Plasmas*; Academic: New York, 1974. Stoneham, A. M. *Rev. Mod. Phys.* **1969**, *41*, 82.
(6) Laird, B. B.; Skinner, J. L. *J. Chem. Phys.* **1989**, *90*, 3274; **1989**, *90*, 3880.
(7) Loring, R. F. *J. Chem. Phys.* **1990**, *92*, 1598. Shemetulskis, N. E.; Loring, R. F. *J. Chem. Phys.* **1990**, *95*, 4756.
(8) Simon, S. H.; Dobrosavljevic, V.; Stratt, R. M. *J. Chem. Phys.* **1990**, *93*, 2640.
(9) Saven, J. G.; Skinner, J. L. *J. Chem. Phys.* **1993**, *99*, 4391.
(10) Abella, I. D.; Kurnit, N. A.; Hartmann, S. *Phys. Rev.* **1966**, *A141*, 391. Mossberg, T.; Flushberg, A.; Kachru, R.; Hartmann, S. R. *Phys. Rev. Lett.* **1979**, *42*, 1665.
(11) (a) Hesselink, W. H.; Wiersma, D. A. *Ibid.* **1979**, *43*, 1991. (b) Nibbering, E. T. J.; Wiersma, D. A.; Duppen, K. *Phys. Rev. Lett.* **1991**, *66*, 2464.
(12) (a) Becker, P. C.; Fragnito, H. L.; Bigot, J.-Y.; Brito-Cruz, C.; Fork, R. L.; Shank C. V. *Phys. Rev. Lett.* **1989**, *63*, 505. (b) Bigot, J.-Y.; Portella, M. T.; Schoenlein, R. W.; Bardeen, C. J.; Migus, A.; Shank, C. V. *Phys. Rev. Lett.* **1991**, *66*, 1138.
(13) (a) Allen, L.; Eberly, J. H. *Optical Resonance, Two-Level Atoms*; Wiley: New York, 1975. (b) Shen, Y. R. *The Principles of Nonlinear Optics*; Wiley: New York, 1984. Mukamel, S. *Annu. Rev. Phys. Chem.* **1990**, *41*, 647.
(14) Cho, M.; Fleming, G. R. *J. Chem. Phys.* **1993**, *98*, 2848.
(15) Weiner, A. M.; De Silvestri, S.; Ippen, E. P. *J. Opt. Soc. Am.* **1985**, *B2*, 654. Weiner, A. M.; De Silvestri, S.; Ippen, E. P. In *Ultrafast Phenomena IV*; Austin, D. H., Eisenthal, K. B., Eds.; Springer-Verlag: Berlin, 1984; pp 230–232.
(16) Duppen, K.; Wiersma, D. A. *J. Opt. Soc. Am.* **1986**, *B3*, 614. Wiersma, D. A.; Duppen, K. *Science* **1987**, *237*, 1147.
(17) Maroncelli and co-workers report an inhomogeneous width of 1100 cm^{-1} (FWHM) for Coumarin 153 in propanol resulting from the distribution of solvent environments. Fee, R. S.; Maroncelli, M. *Chem. Phys.*, in press. Fee, R. S.; Milsom, J. A.; Maroncelli, M. *J. Phys. Chem.* **1991**, *95*, 5170.
(18) Nadler, W.; Marcus, R. A. *Chem. Phys. Lett.* **1988**, *144*, 24.
(19) Stein, A. D.; Fayer, M. D. *J. Chem. Phys.* **1992**, *97*, 2948. Stein, A. D.; Peterson, K. A.; Fayer, M. D. *J. Chem. Phys.* **1990**, *92*, 5622.
(20) Small, G. J.; Hayes, J. M.; Silbey, R. J. *J. Phys. Chem.* **1992**, *96*, 7499.
(21) Tanimura, Y.; Mukamel, S. *J. Chem. Phys.* **1993**, *99*, 9496.
(22) Tanimura, Y.; Mukamel, S. *Phys. Rev.* **1993**, *E47*, 118.
(23) Chesnoy, J.; Mokhtari, A. *Phys. Rev.* **1988**, *A38*, 3566. Walmsley, I. A.; Mitsunaga, M.; Tang, C. L. *Phys. Rev.* **1988**, *A38*, 4681. Scherer, N. F.; Ziegler, L. D.; Fleming, G. R. *J. Chem. Phys.* **1992**, *96*, 5544.
(24) Rosenthal, S. J.; Xie, X.; Du, M.; Fleming, G. R. *J. Chem. Phys.* **1991**, *95*, 4715.
(25) Maroncelli, M.; Fleming, G. R. *J. Chem. Phys.* **1988**, *89*, 5044. Maroncelli, M. *J. Chem. Phys.* **1991**, *94*, 2084. Carter, E. A.; Hynes, J. T. *J. Chem. Phys.* **1991**, *94*, 5961. Perera, L.; Berkowitz, M. L. *J. Chem. Phys.* **1992**, *97*, 5253. Neria, E.; Nitzan, A. *J. Chem. Phys.* **1992**, *96*, 5433.